Polyhedron 205 (2021) 115234

Contents lists available at ScienceDirect

Polyhedron

journal homepage: www.elsevier.com/locate/poly

Oxygen atom transfer catalysis by dioxidomolybdenum(VI) complexes of pyridyl aminophenolate ligands

Md Kamal Hossain [a,b,*], Jörg A. Schachner [c], Matti Haukka [d], Michael G. Richmond [e], Nadia C. Mösch-Zanetti [c], Ari Lehtonen [f], Ebbe Nordlander [a,*]

[a] Chemical Physics, Department of Chemistry, Lund University, P.O. Box 124, SE-22100 Lund, Sweden
[b] Department of Chemistry, Jahangirnagar University, Savar Dhaka-1342, Bangladesh
[c] Institute of Chemistry, Inorganic Chemistry, University of Graz, Schubertstrasse 1, 8010 Graz, Austria
[d] Department of Chemistry, P.O. Box 35, University of Jyväskylä, FI-40014 Jyväskylä, Finland
[e] Department of Chemistry, University of North Texas, 1155 Union Circle #3057070, Denton, TX 76203, USA
[f] Inorganic Materials Chemistry Research Group, Laboratory of Materials Chemistry and Chemical Analysis, Department of Chemistry, University of Turku, 20014 Turku, Finland

ARTICLE INFO

Article history:
Received 8 February 2021
Accepted 19 April 2021
Available online 21 April 2021

Keywords:
Molybdenum
Tripodal tetradentate ligand
Epoxidation
Oxygen atom transfer

ABSTRACT

A series of new cationic dioxidomolybdenum(VI) complexes $[MoO_2(L^n)]PF_6$ (**2**–**5**) with the tripodal tetradentate pyridyl aminophenolate ligands HL^2-HL^5 have been synthesized and characterized. Ligands HL^2-HL^4 carry substituents in the 4-position of the phenolate ring, *viz.* Cl, Br and NO_2, respectively, whereas the ligand HL^5, *N*-(2-hydroxy-3,5-di-*tert*-butylbenzyl)-*N*,*N*-bis(2-pyridylmethyl)amine, is a derivative of 3,5-di-*tert*-butylsalicylaldehyde. X-ray crystal structures of complexes **2**, **3** and **5** reveal that they have a distorted octahedral geometry with the bonding parameters around the metal centres being practically similar. Stoichiometric oxygen atom transfer (OAT) properties of **5** with PPh_3 were investigated using UV–Vis, ^{31}P NMR and mass spectrometry. In CH_2Cl_2 solution, a dimeric Mo(V) complex $[(\mu\text{-}O)\{MoO(L^5)\}_2](PF_6)_2$ **6** was formed while in methanol solution an air-sensitive Mo(IV) complex $[MoO(OCH_3)(L^5)]$ **7** was obtained. The solid-state structure of the μ-oxo bridged dimer **6** was determined by X-ray diffraction. Complex **7** is unstable under ambient conditions and capable of reducing DMSO, thus showing reactivity analogous to that of DMSO reductases. Similarly, the OAT reactions of complexes **2**–**4** also resulted in the formation of dimeric Mo(V) and unsaturated monomeric Mo(IV) complexes that are analogous to complexes **6** and **7**. Catalytic OAT at 25 °C could also be observed, using complexes **1**–**5** as catalysts for oxidation of PPh_3 in deuterated dimethylsulfoxide (DMSO d_6), which functioned both as a solvent and oxidant. All complexes were also tested as catalysts for sulfoxidation of methyl-*p*-tolylsulfide and epoxidation of various alkene substrates with *tert*-butyl hydroperoxide (TBHP) as an oxidant. Complex **1** did not exhibit any sulfoxidation activity under the conditions used, while **2**–**5** catalyzed the sulfoxidation of methyl-p-tolylsulfide. Only complexes **2** and **3**, with ligands containing halide substituents, exhibited good to moderate activity for epoxidation of all alkene substrates studied, and, in general, good activity for all molybdenum(VI) catalysts was only exhibited when *cis*-cyclooctene was used as a substrate. No complex catalysed epoxidation of *cis*-cyclooctene when an aqueous solution of H_2O_2 was used as potential oxidant.

1. Introduction

Mononuclear molybdenum enzymes are widely distributed in nature, and they are generally involved in oxygen atom transfer reactions to or from biological oxygen acceptors/donors [1–3]. These enzymes also contribute to the carbon, nitrogen, and sulfur cycles and their active sites contain an organic cofactor which consists of a molybdenum atom and one or two organic pterin derivatives [4,5]. The mononuclear molybdenum enzymes can be divided into two subcategories - hydroxylases and oxotransferases - under the Hille classification [3]. The latter class can be subdivided into two families based on their structures, *i.e.* the sulfite oxidase (SO) and DMSO reductase (DMSOR) families [3].

A number of complexes have been studied as structural and/or functional models for molybdenum-containing oxotransferase enzymes that catalyse oxygen atom transfer (OAT) reactions

* Corresponding author at: Chemical Physics, Department of Chemistry, Lund University, P.O. Box 124, SE-22100 Lund, Sweden (Md. Kamal Hossain).
E-mail address: Ebbe.Nordlander@chemphys.lu.se (E. Nordlander).

https://doi.org/10.1016/j.poly.2021.115234
0277-5387/

[1,2,6–13]. The OAT reactions between phosphines and oxygen donors have been studied as models for biological reactions. The generally accepted mechanism for oxygen atom transfer to a phosphine proceeds via bonding between the phosphine and one of the oxo ligands which leads to a transient intermediate, and concomitant bridged electron transfer to the molybdenum center [14,15]. This general type of mechanism – for both oxidative and reductive OAT - has been studied and is strongly supported by numerous computational studies [16–19]. Oxidomolybdenum species containing N-, O- and S-donor ligands have been studied extensively as catalysts for OAT reactions [20–24].

Sulfoxides are important synthons for the synthesis of natural and artificial compounds and are used in medicinal chemistry [25–27]. Similarly, epoxides are valuable intermediates and targets in laboratory synthesis, and are important feedstocks in pharmaceutical, agrochemical and chemical industry [28–31]. Molybdenum-based catalysts are effective for the epoxidation of unfunctionalized olefins. Oxidomolybdenum complexes also have potential applications in the field of asymmetric epoxidation of chiral alkenes [32,33]. We are interested in the development of new, relatively inexpensive molybdenum(VI) based catalysts for catalytic oxidation reactions that are also significant in the chemical industry, such as sulfoxidation and epoxidation reactions [34–39]. We have also investigated the reactivities of molybdenum oxo complexes as bioinspired models for molybdenum-containing OAT enzymes [1,40].

There are previous reports on metal complexes with phenols carrying di-(2-picolyl)amine substituents at the ortho positions. For example, the tripodal ligands HL^1-HL^5 (Fig. 1) are known to readily form coordination compounds with Mg(II), Zn(II) [41], Fe (III) [42], V(V) [43], Eu(III) and Yb(III) [44]. The catalytic activities of complexes based on these ligands have been studied, e.g. the catechol dioxygenase and proton reduction properties of iron complexes [42,48], ring-opening polymerization of ε-caprolactone by zinc complexes [41], and catalytic activities for ethylene polymerization of vanadium complexes [43].

We have previously reported the dioxidomolybdenum(VI) complex **1** of the pyridylaminophenolate ligand HL^1 but its catalytic oxidation chemistry was not studied [1]. In this contribution, we present the syntheses and characterizations of four MoO_2(VI) complexes (**2**–**5**) containing related pyridyl aminophenolate ligands with different electron-donating and -withdrawing groups on the ligand backbone (Fig. 1 and Scheme 1), and explore the catalytic applications of **1**–**5** in oxygen atom transfer, sulfoxidation and epoxidation reactions with various substrates. A dinuclear oxido-bridged molybdenum(V) complex **6** and a mononuclear MoO(IV) complex **7** were isolated as products in the OAT reactions of **5** with PPh_3.

2. Results and discussion

2.1. Synthesis and characterization of complexes

The tripodal tetradentate pyridylaminophenolate ligands HL^1-HL^5 were prepared in a straightforward manner by reductive

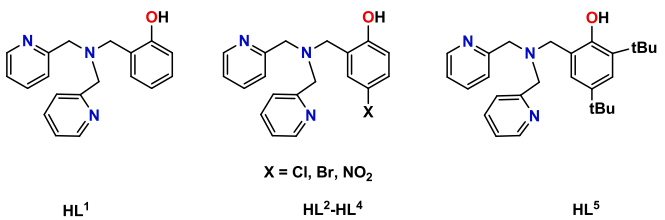

Fig. 1. Structures of the tripodal ligands employed in the study.

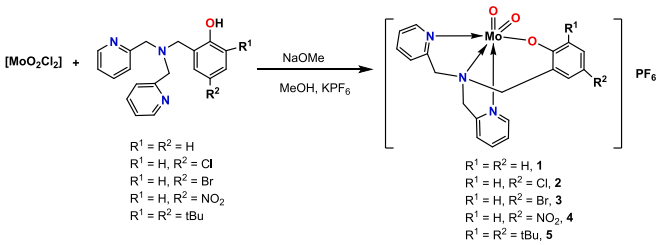

Scheme 1. Synthetic route of dioxidomolybdenum(VI) complexes **1**–**5**.

amination, a known procedure starting from di-(2-picolyl)amine and the corresponding salicylaldehyde [42,45,46]. Complex **1** was prepared following a published procedure [1], and the other complexes were synthesised analogously. The reaction of $[MoO_2Cl_2]$ with the tripodal ligands HL^2-HL^5 in the presence of NaOMe and KPF_6 in methanol results in the formation of cationic complexes of the type $[MoO_2(L^n)]^+$ (Scheme 1). In each case, the reaction mixture was diluted with diethyl ether and hexane, filtered through a pad of Celite and evaporated to dryness. Crystallisation from methanol gave pure products in 61–75% yields. Complexes **2**–**5** can also be prepared in similar yields (*ca.* 60–75%) by the reaction of HL^2-HL^5 with other molybdenum precursors, such as $[MoO_2(acac)_2]$ or $[MoO_2Cl_2(dmso)_2]$, following the synthetic protocol described above.

The tripodal ligands HL^1-HL^5 can coordinate to the *cis*-dioxidomolybdenum moiety to form two possible configurational isomers, *i.e.* the methylpyridyl groups may be coordinated *cis* or *trans* to each other. One isomer (isomer **A** in Fig. 2; X = H) has these two pyridyl side-arms donor located in *trans* positions to the phenolate and oxido ligands whereas in another isomer (**B**), the phenolate moiety is *trans* to one oxido ligand. Previous studies on Mo and Fe complexes, for example $[MoO_2(L^1)]^+$ [1], $[FeCl_2(L^1)]$ [46,47], and $[FeCl_2(L^4)]$[48] have shown that such ligands tend to coordinate with the pyridyl arms *cis* to each other (Fig. 2, isomer A), a feature that was confirmed by DFT calculations. The structures of the two isomers based on complex **1**[1] were optimized and these optimized structures are shown in Fig. 2. Isomer **A** was computed to be 9.3 kcal/mol more stable than isomer **B**. As already mentioned, complex **1** is a known compound, but was prepared during this work to evaluate its catalytic efficiency.

The solubility in common solvents varies with the electron-withdrawing and electron-releasing substituents on the phenyl rings. Complexes **2**–**4** are readily soluble in methanol and acetonitrile but they are less soluble in chlorinated solvents ($CHCl_3$, CH_2Cl_2). Complex **5** is soluble in both polar and non-polar organic solvents due to the presence of the *tert*-butyl substituents. All complexes were characterized by ^1H, ^{13}C, ^{31}P and ^{19}F NMR, IR spectroscopy and mass spectrometry (Spectroscopic data are given in the Supplementary Information, Figs. S1-S11). The structures of complexes **2**, **3** and **5** were also verified by single-crystal X-ray crystallography (*vide infra*). As anticipated, complexes **2**–**5** have relatively similar NMR and IR spectra. The infrared spectra of all studied complexes showed two strong bands around 880–905 and 910–950 cm^{-1} which are assigned to asymmetric and symmetric M=O stretches, respectively [49–52]. The ^1H NMR spectra were recorded in CD_3OD solutions while the chemical shifts for the phenolate ring protons as well as for the two inequivalent pyridine rings were seen around 6.5–9.3 ppm as 11 sharp signals for **2**–**4** and 10 resonances for **5** (*cf.* ref 1). This indicates that the two pyridyl side-arm donors are located in *cis* to each other, so isomer **A** (Fig. 2) is the prevalent species in solution. The chemical shifts for the two *tert*-butyl groups of **5** are within the expected region. The singlets of the six N-CH_2 methylene protons exhibit separated resonances

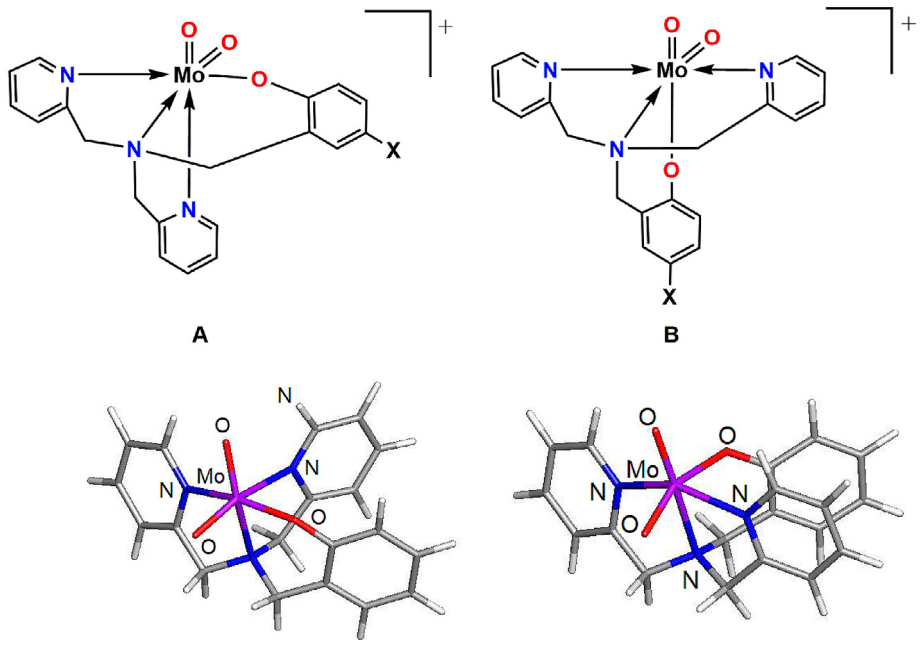

Fig. 2. Two possible configurational isomers for the studied complexes with the DFT-optimized structures of each isomer of complex **1** [1].

within the range 4–6 ppm which is consistent for all three pendant arms of the ligand being inequivalent. The NMR spectra match well with the solid-state structures (*vide infra*).

When the reaction of **5** with PPh_3 in dichloromethane was studied under N_2 atmosphere, the solution turned red and then the colour changed to dark purple. After half an hour, the solution was filtered and the dark purple solid was collected. The ^1H NMR spectrum of the complex showed rather complicated and broad signals indicating the formation of a paramagnetic Mo(V) complex. The UV–vis spectrum is consistent with the dimeric complex prepared previously by the reaction of **1** under similar conditions [1]. The formation of the dark purple Mo(V) dimer $[(\mu\text{-O})\{MoO(L^5)\}_2](PF_6)_2$ **6** was verified by the observation of a peak in its electrospray high resolution mass spectrum that matches the expected empirical formula (see Fig. S12 and Scheme 2). Single crystal X-ray crystallographic analysis revealed that **6** is a dinuclear oxo-bridged Mo(V) complex (see Fig. S13 and crystallographic data summarized in Table S1).

When the reaction of **5** with 1.5 equivalents of PPh_3 was studied in a methanol solution, the yellow colour of the solution turned red within fifteen minutes. The reaction led to the formation of $OPPh_3$ (as identified by ^{31}P NMR) and a reduced oxidomolybdenum(IV) complex. The red complex was identified as the mononuclear complex $[Mo(IV)O(OCH_3)(L^5)]$ **7** through a high resolution mass spectrum, which shows a molecular ion peak $[M]^+$ with a characteristic molybdenum pattern (see Fig. S14). The red complex reduces biological oxygen donors such as dimethyl sulfoxide (DMSO) albeit in a slow reaction, as evidenced by the reformation of **5** seen by UV–Vis spectroscopy. This phenomenon is also closely related with our previous studies [1]. Unfortunately, while the reduced oxidomolybdenum(IV) complex **7** was found to be comparatively stable in DMSO solution under anaerobic conditions at room temperature, all attempts to isolate the desired complex **7** were unsuccessful, leading only to the formation of small amounts of the dark purple Mo(V) oxo dimer **6** (*vide supra*), as previously observed also for the analogous reduced oxidomolybdenum(IV) complex formed from **1** [1].

The analogous oxygen atom transfer reactions to PPh_3 were studied under equivalent conditions for complexes **2**–**4** in both dichloromethane and methanol. The results were analogous to the above-mentioned reactions; in the potentially coordinating solvent methanol, red unstable Mo(IV) complexes of the general formula $[MoO(OCH_3)(L)]$ (L = pyridine aminophenolate ligand) could be identified, while in the usually non-coordinating solvent dichloromethane, purple $[(\mu\text{-O})\{MoO(L)\}_2]^{2+}$ complexes were formed. The Mo(V) dimers and unstable $Mo(IV)O(OCH_3)$ complexes were characterized by ^1H NMR and UV–vis spectroscopy, respectively, and the spectra correspond to those for **6** and **7**.

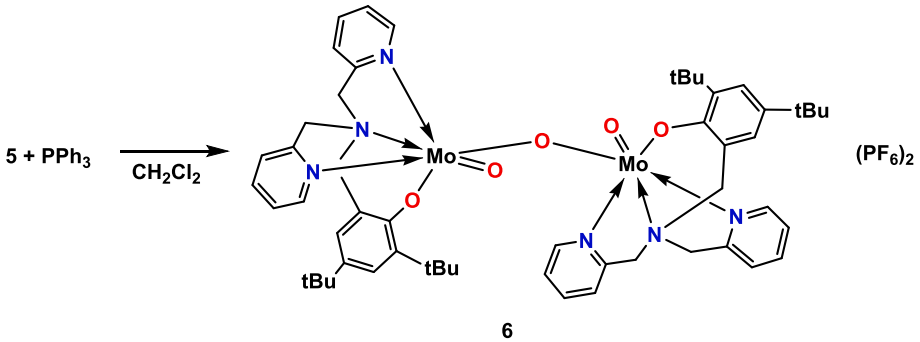

Scheme 2. Synthesis of Mo(V) dimer $[(\mu\text{-O})\{MoO(L^5)\}_2](PF_6)_2$ **6.**

Electrospray ionization (ESI) mass spectrometry was used for the characterization of complexes **2**–**7**. The mass spectrum of **2** shows a molecular ion $[M]^+$ peak at $m/z = 468$ and a ligand molecular ion at $[HL^2 + H]^+$ at $m/z = 340$. Similarly, complexes **3** and **4** exhibit peaks at $m/z = 512$ and $m/z = 479$, respectively, which can be assigned to the molecular ion $[M]^+$ peak. The ligand molecular ions were observed at $[HL^3 + H]^+$ at $m/z = 384$ and $[HL^4 + H]^+$ at $m/z = 351$, accordingly. Complex **5** is identified as molecular ion $[M]^+$ peak at $m/z = 546$ and the corresponding ligand peak $[HL^5 + H]^+$ at $m/z = 418$. In addition, in solution **5** shows a Mo(V) dimeric complex as molecular ion $[(\mu\text{-O})\{MoO(L^5)\}_2 + NaOMe]^+$ at $m/z = 1126$ due to the samples injected as dichloromethane solutions, preceded and followed by methanol. The characteristic molecular ion peaks for complexes **6** and **7** are at $m/z = 1073$ and $m/z = 561$, respectively.

2.2. Description of the X-ray crystal structures

Single crystals of **2**, **3** and **5** suitable for crystallographic analysis were obtained from concentrated methanol solutions at − 4 °C and their solid-state structures were determined by X-ray diffraction. The crystallographic data together with the collection and refinement parameters for complexes are summarized in the Supplementary Material, Table S2. Selected bond distances and angles are listed in the Supplementary Material, Table S3. In all structures, there is one cationic complex and one PF_6^- anion in the asymmetric unit. The molecular structure of **2** is illustrated in Fig. 3, and the analogous structures of **3** and **5** are shown in the Supplementary Material as Figs. S15 and S16, respectively. All complexes have a distorted octahedral geometry in which the two *cis*-positioned oxido ligands bind strongly to the Mo(VI) ion, while the geometrical parameters are very similar. The two pyridyl rings are almost perpendicularly aligned relative to each other in complexes **2**, **3** and **5;** the N(1)-Mo(2)-N(3) angle is 84.35(10)° for **2**, 84.15(9)° for **3** and 83.38(7)° for **5**, respectively. In the three complexes, the three oxygen donor atoms are in the *fac* arrangement of a distorted octahedron where all three donor groups are about 105°-108° apart. The structures confirm that two nitrogen atoms in the pyridine rings of the chelating amine bis-pyridine phenolate ligand are located in *cis* positions with the N(1)-Mo(1)-N(2) and N(3)-Mo(1)-N(2) bond angles are 70.87(10)° and 71.98(9)° for **2**, 70.86(9)° and 71.70(8)° for **3** and 71.32(7)° and 71.91(6)° for **5**, respectively. One pyridyl group is coordinated *trans* to the aryloxide group and the other one is *trans* to the oxido ligand O3 while the central amine nitrogen N2 of the ligand backbone is coordinated *trans* to the terminal oxido ligand O2. The bond distances of the oxido ligands O2 and O3 and the O(2)–Mo(1)–O(3) angle of complexes **2**, **3** and **5** are within the expected range and comparable with previously reported six-coordinate dioxidomolybdenum complexes [1,21]. The Mo(1)–N(3) bond distance, 2.298(3) Å for **2**, 2.302(2) Å for **3** and 2.3120(18) Å for **5,** respectively, that is slightly longer than the Mo(1)–N1 bond distance, 2.183(3) Å for **2**, 2.181(2) Å for **3** and 2.192(2) Å for **5,** respectively due to the strong *trans* influence of the oxido ligand compared to the phenolate moiety. The bond distances Mo(1)–N1 and Mo(1)–N(3) are seemingly shorter than the Mo(1)–N(2) bond distance (2.322(3) Å for **2**, 2.332(2) Å for **3** and 2.3116(18) Å for **5,** respectively) indicating that the central nitrogen atom of the ligand backbone is coordinated more weakly to the Mo centre than the pyridine *N*-donors. All these Mo–N distances are shorter than in previously reported $[MO_2(L\text{–}O_2)]$ complexes with Mo–N bond lengths > 2.30 Å, where $L\text{–}O_2^{2-}$ is the corresponding tripodal ligand with one pyridyl and two phenolate rings [53].

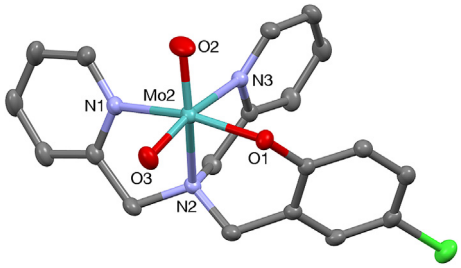

Fig. 3. Mercury diagram of the molecular structure of $[MoO_2(L^2)]^+$ (**2**) showing parts of the numbering schemes. Thermal ellipsoids are plotted at the 30% probability level. Hydrogen atoms and the hexafluorophosphate anions are omitted for clarity of presentation.

Single crystals of **6** were grown from acetonitrile solution with excess of $NaBPh_4$ in order to ascertain the dimeric framework. Unfortunately, the very thin needle-shaped crystals gave weak diffraction patterns with Mo-Kα radiation leading to the high R-values because of the lack of the good quality data set. However, the dimeric nature of **6** could be proven (see Fig. S2).

3. Catalysis studies

3.1. Catalytic oxygen atom transfer

Catalytic oxygen atom transfer (OAT) properties of complexes **1**–**5** to the non-biological substrate triphenylphosphine were investigated (Scheme 3) in deuterated dimethyl sulfoxide (DMSO d_6) while the reaction course was followed by ^{31}P NMR. Preliminary experiments showed that reactions are very fast with catalyst loadings of 1–10 mol- % at 65 °C. Under such conditions, PPh_3 was fully oxidized into $OPPh_3$ (as seen by ^{31}P NMR at around 27 ppm) within 1–2 min with all studied complexes. To further probe the catalytic profiles of the catalysts, the reactivity screening was carried out with low catalyst loadings (1 mol %) at 25 °C. Complex **2** exhibited the fastest reaction rate with a half-life of approximately 5 min compared to complexes **1** and **3**, which showed the half-lives of approximately 15 min. The sterically more hindered complex **5** showed a lower rate of reaction (half-life approx. 1 h) under similar conditions. Under these experimental conditions, PPh_3 was formed in a 98% yield with catalyst **2** after 1 h while with catalysts **1**, **3** and **5**, 3 hrs were required to reach a 95% yield. The calculated turn-over frequencies (TOFs) for complexes **1**, **2**, **3** and **5** were of the same order of magnitude, ranging from 104 h^{-1} to 296 h^{-1}, after an induction period of around 15 min whereas **4** showed the lowest activity (TOF = 40 h^{-1}). The data obtained in the OAT experiments is summarized in Table 1.

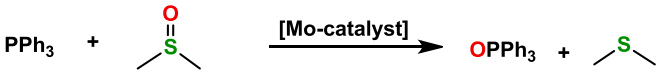

Scheme 3.

3.2. Catalytic sulfoxidation

The oxidation of methyl-*p*-tolyl sulfide with two equivalents of *tert*-butyl hydroperoxide as the oxygen atom source was studied using dioxidomolybdenum complexes **1**–**5** as catalysts (Scheme 4). The reactions were run under atmospheric conditions in deuterated methanol solution and the reaction course was monitored by ^1H NMR. In control experiments that were run in the absence of catalysts no sulfoxide was obtained. Complex **1** was found to be inactive as a sulfoxidation catalyst under the conditions employed. The reason for this lack of activity is not clear; it may be that the Mo(VI) peroxo complex that is expected to be formed during the reaction is too unstable. In other experiments, the catalytic reactions started immediately without any noticeable

Table 1
Catalytic OAT of triphenylphosphine by dimethylsulfoxide at 25 °C with 1 mol-% of catalysts.

Catalyst	Yield (%)[a]	TON [b]	TOF (h^{-1}) [c]
1	95	52	208
2	98[d]	74	296
3	98	60	240
4	51	10	40
5	92	26	104

[a] Yield of the product measured by ^{1}H NMR after 3 h. [b]TON calculated after 15 min of reaction as (mol product) (mol catalyst)$^{-1}$. [c]TOF calculated after 15 min of reaction as (mol product) (mol catalyst)$^{-1}$ (t/h)$^{-1}$. [d]Yield of the product measured by ^{1}H NMR after 1 h.

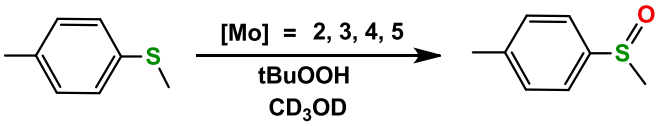

Scheme 4.

induction times. After a one-hour reaction, the highest yield (97%) of a sulfoxide product was observed with catalyst **4** and the lowest yield (60%) was obtained for **3**. Moreover, the sulfoxidations were found to be selective, without any sign of the formation of sulfone. All values obtained in the sulfoxidation experiments are listed in Table 2.

Table 2
Catalytic sulfoxidation of methyl-*p*-tolylsulfide by *tert*-BuOOH at 25 °C.

Catalyst	Yield (%)[a]	TON[b]	TOF (h^{-1}) [c]
1	–	–	–
2	70	30	124
3	60	23	92
4	97	77	308
5	91	59	236

Reaction conditions: 1 mol % of catalysts (**1**–**5**), 2.0 equivalents of *tert*-BuOOH at 25 °C. [a]Yield of the product measured by ^{1}H NMR after an hour. [b]TON calculated after 15 min of reaction as (mol product) (mol catalyst)$^{-1}$. [c]TOF calculated after 15 min of reaction as (mol product) (mol catalyst)$^{-1}$ (t/h)$^{-1}$.

3.3. Catalytic epoxidation

Complexes **1**–**5** were tested as catalysts for the epoxidation of five olefinic substrates, viz. *cis*-cyclooctene **S1**, 1-octene **S2**, styrene **S3**, limonene **S4** and α-terpineol **S5** (Fig. 4). In the case of **S4** and **S5**, the racemic mixtures of the D- and L-enantiomers were used. The reactions were carried out with three equivalents of *tert*-butylhydroperoxide (TBHP) as an oxidant and 1 mol % catalyst loadings. The reactions were run at 50 °C in $CHCl_3$ solutions and conversions to epoxides were followed by GC–MS.

As expected, all five molybdenum complexes did show catalytic activity with **S1,** albeit with highly different activities (Table 3). Whereas the two halogenated complexes **2** and **3** showed complete conversion of cyclooctene to epoxide within seven and four hours respectively, complexes **1**, **4** and **5** only showed low to moderate activity with cyclooctene **S1** (Table 3). For the more challenging substrates **S2-S5**, again only complexes **2** and **3** showed some catalytic activity (Table 3). For 1-octene **S2**, complexes **1**, **4** and **5** showed no conversion of substrate, for substrates **S3-S5**, complexes **1**, **4** and **5** displayed conversion of substrate, but low selectivity to epoxide due to over-oxidation despite the relatively low excess of oxidant. For example, in styrene epoxidation phenyl acetaldehyde and benzaldehyde were formed; for limonene and α-terpineol formation of the respective ketones was observed in GC–MS spectrometry (Table 3).

From the observed catalytic activities in olefin epoxidation, it can be concluded that complexes **1**–**5** are very sensitive to the substituents present in the ligand backbone. The presence of halide substituents like Cl in complex **2** and Br in complex **3** results in epoxidation catalysts with reasonable activity. The absence of substituents, as in **1**, or the presence of ^{t}Bu-groups (**5**) or a NO_2-group (**4**) do not result in active epoxidation catalysts.

Using Hammett σ_p constants as qualitative indicators of the relative electron-withdrawing/electron-donating properties of the different substituents, it may be noted that the most strongly electron-withdrawing substituent (NO_2, complex **4**) leads to the best performance in sulfoxidation of methyl-*p*-tolylsulfide (Table 2) but the worst performance (with the exception of non-substituted HL1, complex **1**) in catalytic epoxidations (Table 3). It may also be noted that the chloro-substituted complex **2** and the bromo-substituted complex **3** show the same catalytic activities, within experimental error of detection, with chlorine and bromine possessing identical σ_p constants. These two complexes with weakly

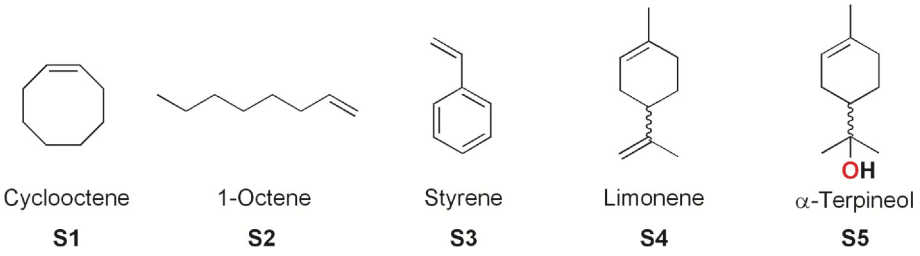

Fig. 4. Olefinic substrates used for epoxidation experiments. In the cases of **S4** and **S5**, racemic mixtures of the R- and S-isomers were used.

Table 3
Conversion of substrate (selectivity to epoxide) for complexes **1**–**5**.

[%]	**1**	**2**	**3**	**4**	**5**
cyclooctene, **S1**	48 (81)	>95 (99)[a]	>95 (99)[b]	59 (97)	86 (93)
1-octene, **S2**	no conv.	33 (92)	29 (97)	no conv.	no conv.
styrene, **S3**	unsel.	64 (22)	59 (63)	unsel.	unsel.
limonene, **S4**	unsel.	>95 (35)	>95 (47)	unsel.	unsel.
α-terpineol, **S5**	unsel.	70 (22)	88 (53)	unsel.	unsel.

General conditions: 1 mol % catalyst, 0.5 mL $CHCl_3$, 50 °C, 3 equiv. TBHP, conversion of substrate (selectivity to epoxide) after 24 h; no conv. = no substrate conversion, unsel. = selectivity to epoxide < 10%; [a] max. yield of epoxide reached after 7 h; [b] max. yield of epoxide reached after 4 h.

electron-withdrawing substituents exhibit the best catalytic performances in epoxidation but are the two worst (bar complex **1**) catalysts for sulfoxidation. The mediocre performance of complex **4** in phosphine oxidation runs counter to earlier observations where the presence of a strongly electron-withdrawing substituent (*e.g.* $-NO_2$) in *para*-position on a molybdenum-coordinating phenolate leads to increased rate of phosphine oxidation [54,55]. This suggests that it is not simply the electronic influence of the substituent that is responsible for catalyst activity in the present study. Other factors, like catalyst stability in the presence of a large amount of oxidant, may also play a vital role. The poor catalytic performance by complex **1** is puzzling and difficult to rationalize.

4. Conclusion

Five tripodal tetradentate pyridyl aminophenolate ligands, with varying electronic and steric properties depending on the nature of the substituents on the phenolate ring were used to prepare a series of monomeric molybdenum(VI) complexes of the general formula $[MoO_2(L^n)]PF_6$ (**1**–**5**). In addition, the dimeric molybdenum (V) complex $[(\mu\text{-}O)\{MoO(L^5\text{–}O)\}_2](PF_6)_2$ (**6**) was isolated and characterized as a disproportionation product formed upon oxotransfer from $[MoO_2(L^5)]PF_6$ (**5**) In the catalytic oxygen atom transfer reaction (OAT) from DMSO to PPh_3, complex **2** exhibited significant activity compared with **1** and **3**, whereas **5** showed very poor conversion, which is attributed to the steric hindrance exerted by the *tert*-butyl substituents of the ligand. Compound **4** with a nitro substituent in the phenolate showed the lowest activity in the OAT experiment. The major difference of structure related activity was observed in the sulfoxidation reaction, where catalyst **4** shows the highest conversion while **1** was found to be completely inactive. In the epoxidation of *cis*-cyclooctene, the halogenated catalysts **2** and **3** showed full conversion to epoxide while complexes **1**, **4** and **5** showed low to moderate activity. For the more demanding olefinic substrates, only complexes **2** and **3** showed some activity while **1**, **4** and **5** were practically inactive.

5. Experimental section

5.1. General procedures and materials

Unless otherwise noted, all experiments involving metal complexes were carried out under atmospheric conditions with standard laboratory equipment. Commercial grade reagents and solvents were purchased from commercial suppliers (Fisher Scientific and Sigma-Aldrich) and used without further purification. The ligands HL^1-HL^5 were synthesized according to published procedures [42,45,46]. The ^1H, ^{13}C, ^{31}P and ^{19}F NMR spectra were recorded on a Varian Inova 500 MHz instrument spectrometer. NMR chemical shifts are reported in ppm using deuterated methanol or chloroform as solvents, and referenced to the residual solvent peak as internal standard; ^{31}P NMR chemical shifts are referenced to external H_3PO_4. Peaks are reported as singlet (s), doublet (d), doublet of doublets (dd), triplet (t), heptet (hept) and multiplet (m or unresolved), coupling constants are given in Hz. The IR spectra were measured with a Bruker Optics, Vertex 70 spectrophotometer with a diamond ATR setup; resonances are listed with wave numbers (cm^{-1}) and intensities (br = broad, vs = very strong, s = strong, m = medium, w = weak). Mass spectrometry was performed on Waters ZQ 4000 or Waters QTof Xevo-G2 spectrometers. The samples were injected as MeCN and MeOH solutions for **6** and **7** and measured on a Waters QTof Xevo-G2 spectrometer. Results are denoted as cationic mass peaks; unit is the mass/charge ratio. Gas chromatography mass spectroscopy (GC–MS) measurements were performed with an Agilent 7890 A gas chromatograph (column type, Agilent 19091 J–433), coupled to an Agilent 5975C mass spectrometer.

5.2. Preparation of complexes **2**–**5**

General procedure: The complexes were prepared by the reaction of $[MoO_2Cl_2]$ (1.0 mmol) with the respective ligand HL^n (1.0 mmol), KPF_6 (1.20 mmol) and NaOMe (1.25 mmol) in 20 mL of methanol. The reaction mixture was stirred for 4 h and placed in a freezer overnight to yield a precipitate which was removed by filtration. Diethyl ether (10 mL) and hexane (10 mL) were added to the filtered solution to precipitate more white solid, which was also removed by filtration through a Celite pad. The yellow solution was kept at − 4 °C overnight. Removal of the solvent at reduced pressure afforded the relevant product which was dried under vacuum. The pure products were recrystallized from concentrated methanol solutions at − 4 °C and isolated after a week.

$[MoO_2(L^2)]PF_6$, **2**, orange-red crystals, 0.40 g (65%). ^1H NMR (500 MHz, CD_3OD) δ 9.24 (d, J = 5.2 Hz, 1H), 8.79 (d, J = 5.2 Hz, 1H), 8.29 (t, J = 7.7 Hz, 1H), 7.91 (d, J = 5.2 Hz, 1H), 7.86 (d, J = 5.2 Hz, 1H), 7.72 (d, J = 5.2 Hz, 1H), 7.55 (t, J = 7.7 Hz, 1H), 7.46 (s, 1H), 7.12 (t, J = 7.7 Hz, 2H), 6.52 (d, J = 5.2 Hz, 1H), 5.32 – 5.24 (m, 2H), 4.93 (d, J = 10.9 Hz, 1H), 4.51 (dd, J = 14.3, 9.0 Hz, 2H), 4.22 (d, J = 17.9 Hz, 1H). ^1H NMR (500 MHz, $CDCl_3$) δ 9.16 (d, J = 5.2 Hz, 1H), 8.66 (d, J = 5.2 Hz, 1H), 8.15 (t, J = 7.7 Hz, 1H), 7.95 (d, J = 5.2 Hz, 1H), 7.78 (t, J = 7.7 Hz, 1H), 7.56 (t, J = 7.7 Hz, 1H), 7.42 (t, J = 7.7 Hz, 1H), 7.35 (s, 1H), 7.17 (d, J = 5.2 Hz, 1H), 7.10 (d, J = 5.2 Hz, 1H), 6.52 (d, J = 5.2 Hz, 1H), 5.26 (t, J = 16.6 Hz, 2H), 5.05 (d, J = 14.0 Hz, 1H), 4.48 (dd, J = 32.1, 15.4 Hz, 3H). ^{13}C NMR (126 MHz, CD_3OD) δ 157.87, 156.47, 154.66, 153.52, 151.82, 150.04, 144.04, 142.44, 141.65, 130.39, 127.72, 126.90, 125.02, 123.98, 122.20, 118.89 (Ar-C), 66.54, 60.44 (CH_2). ^{31}P NMR (202 MHz, $CDCl_3$) δ −144.22 (hept, J = 713.4 Hz). ^{19}F NMR (470 MHz, CD_3OD) δ −74.06 (s), −75.57 (s). Selected FT-IR (cm^{-1}) 938 s (Mo = O), 917 s (Mo = O). ESI-MS: m/z = 468 $[2]^+$, 340 $[HL^2 + H]^+$.

$[MoO_2(L^3)]PF_6$, **3**, red crystals, 0.46 g (71%). ^1H NMR (500 MHz, CD_3OD) δ 9.27 (d, J = 5.2 Hz, 1H), 8.82 (d, J = 5.2 Hz, 1H), 8.32 (t, J = 7.7 Hz, 1H), 7.94 (d, J = 5.2 Hz, 1H), 7.90 (t, J = 7.7 Hz, 1H), 7.76 (t, J = 7.7 Hz, 1H), 7.63 (s, 1H), 7.58 (t, J = 7.7 Hz, 1H), 7.29 (d, J = 5.2 Hz, 1H), 7.16 (d, J = 7.9 Hz, 1H), 6.50 (d, J = 8.6 Hz, 1H), 5.31 (dd, J = 14.3, 9.0 Hz, 2H), 4.94 (d, J = 15.4 Hz, 1H), 4.54 (dd, J = 14.3, 9.0 Hz, 2H), 4.25 (d, J = 17.9 Hz, 1H). ^{13}C NMR (126 MHz, CD_3OD) δ 158.47, 157.66, 156.23, 154.68, 153.45, 150.04, 144.05, 141.70, 133.39, 133.24, 126.96, 125.02, 124.41, 122.16, 119.27, 115.01 (Ar-C), 66.56, 60.45 (CH_2). ^{31}P NMR (202 MHz, $CDCl_3$) δ −144.22 (hept, J = 713.4 Hz). ^{19}F NMR (470 MHz, CD_3OD) δ −74.09 (s), −75.59 (s). Selected FT-IR (cm^{-1}) 936 s (Mo = O), 916 s (Mo = O). ESI-MS: m/z = 512 $[3]^+$, 384 $[HL^3 + H]^+$.

$[MoO_2(L^4)]PF_6$, **4,** red crystals, 0.38 g (61%). ^1H NMR (500 MHz, CD_3OD) δ 9.26 (d, J = 5.2 Hz, 1H), 9.13 (d, J = 5.2 Hz, 1H), 8.88 (d, J = 5.2 Hz, 1H), 8.78 (d, J = 5.2 Hz, 1H), 8.61 (t, J = 7.7 Hz, 1H), 8.42 (s, 1H), 8.31 (t, J = 7.7 Hz, 1H), 7.96 (t, J = 7.7 Hz, 1H), 7.75 (t, J = 7.7 Hz, 1H), 7.15 (d, J = 7.9 Hz, 1H), 6.72 (d, J = 8.6 Hz, 1H), 5.34 (t, J = 16.6 Hz, 2H), 5.07 (d, J = 15.4 Hz, 1H), 4.98 (d, J = 15.4 Hz, 1H), 4.62 (d, J = 15.4 Hz, 1H), 4.39 (d, J = 15.4 Hz, 1H). ^{31}P NMR (202 MHz, $CDCl_3$) δ −144.22 (hept, J = 713.4 Hz). ^{19}F NMR (470 MHz, CD_3OD) δ −73.86 (s), −75.36 (s). Selected FT-IR (cm^{-1}) 949 s (Mo = O), 935 s (Mo = O). ESI-MS: m/z = 479 $[4]^+$, 351 $[HL^4 + H]^+$.

$[MoO_2(L^5)]PF_6$, **5**, deep red crystals, 0.52 g (75%). ^1H NMR (500 MHz, $CDCl_3$) δ 9.18 (d, J = 5.2 Hz, 1H), 8.70 (d, J = 5.2 Hz, 1H), 8.16 (td, J = 7.8, 1.5 Hz, 1H), 7.91 (d, J = 5.2 Hz, 1H), 7.78 (td, J = 7.8, 1.5 Hz, 1H), 7.59 (t, J = 7.7 Hz, 1H), 7.40 (t, J = 7.7 Hz, 1H), 7.25 (d, J = 5.2 Hz, 1H), 7.23 (d, J = 5.2 Hz, 1H), 7.13 (d, J = 5.2 Hz, 1H), 5.37 (d, J = 15.4 Hz, 1H), 5.12 (dd, J = 14.3, 9.0 Hz, 2H), 4.65

(d, J = 15.4 Hz, 1H), 4.50 (d, J = 15.4 Hz, 1H), 4.36 (d, J = 15.4 Hz, 1H), 1.31 (s, 9H), 1.20 (s, 9H). ^{13}C NMR (126 MHz, $CDCl_3$) δ 155.56, 155.52, 155.11, 152.54, 150.31, 147.01, 143.79, 141.62, 138.02, 126.90, 126.10, 125.63, 125.58, 124.64, 122.53, 121.27 (Ar-C), 67.43, 62.71, 60.30 (CH_2), 34.97, 34.63 [$C(CH_3)_3$], 31.37, 29.97 (CH_3). ^{31}P NMR (202 MHz, $CDCl_3$) δ −144.22 (hept, J = 713.4 Hz). ^{19}F NMR (470 MHz, $CDCl_3$) δ −71.04 (s), −72.56 (s). Selected FT-IR (cm^{-1}) 921 s (Mo = O), 907 s (Mo = O). UV–vis in MeCN: λ_{max}, nm (ε, $M^{-1}cm^{-1}$): 209 (49166), 275 (11023), 402 (3163). ESI-MS: m/z = 546 [4]$^+$, 418 [HL^5 + H]$^+$, [(μ-O){MoO-(L^5–O)}$_2$ + NaOMe]$^+$ at m/z = 1126.

Preparation of complex [(μ-O){MoO(L^5)}$_2$](PF_6)$_2$, **6**. A solution of PPh_3 (0.038 mmol) in 2 mL of dichloromethane was added to the solution of **5** (0.073 mmol) in 5 mL of dichloromethane under inert atmosphere. The colour of the solution changed from yellow to dark purple within 5 min. After 15 min, a purple solid started to precipitate and 5 mL diethyl ether was added. The product [(μ-O){MoO(L^5)}$_2$](PF_6)$_2$ **6** was isolated by filtration as a dark purple solid (0.025 mmol, 35% yield). UV–vis in MeCN: λ_{max}, nm (ε, $M^{-1}cm^{-1}$): 210 (89723), 265 (29615), 404 (6568), 570 (9111). HRMS: m/z = 1073.3405 [6]$^+$, 1114.3145 [**6** + MeCN]$^+$.

Preparation of complex [MoO(OCH_3)(L^5)], **7**. Complex **5** (0.02 mmol) was dissolved in 5 mL of methanol and PPh_3 (0.03 mmol) was added under nitrogen atmosphere. A red colour appeared immediately upon addition of the PPh_3 to the complex solution. After stirring for 15 min, the UV–Vis and mass data were recorded for **7**. UV–vis in MeOH: λ_{max}, nm (ε, $M^{-1}cm^{-1}$): 227 (20102), 257 (9107), 274 (9080), 393 (1478). HRMS: m/z = 561.1899 [7]$^+$. Finally, the solution was dried under vacuum leading to the isolation of a small quantities of solid product as **6** (*vide supra*).

5.3. Catalytic oxygen atom transfer reactions

The OAT reactions of PPh_3 (0.2 mmol) catalysed by complexes **1**–**5** (0.002 mmol) were run in DMSO d_6 (0.5 mL) at 25 °C. The reaction progress was monitored by ^{31}P NMR using a fifteen-minute interval, measuring the disappearance of a resonance at −6 ppm for PPh_3 and the appearance of a signal for $OPPh_3$ at approx. 27 ppm. The ^{31}P{^{1}H} NMR spectra were externally referenced to 85% H_3PO_4.

5.4. Sulfoxidation reactions

In these experiments, complexes **1**–**5** were tested as catalysts for the oxidation of methyl-*p*-tolyl sulfide at room temperature in CD_3OD solutions using 1:2 M ratios of substrate/*tert*-BuOOH (0.19 M: 0.38 M) and 10 μL of 1,2-dichloroethane was added as an internal standard in a 5 mm NMR tube. The complete selectivity towards the sulfoxide was monitored by ^{1}H NMR spectroscopy at fifteen-minute intervals. The reaction rates were estimated on the basis of the integrated intensities of substrate and product spectra. In the sulfoxidation test, the sulfide methyl singlet at 2.27 was turned to the sulfoxide methyl singlet at 2.75 ppm.

5.5. Epoxidation of olefins

A Heidolph Parallel Synthesizer 1 was used. In a typical epoxidation experiment 2–3 mg of the respective catalyst was dissolved in 0.5 mL of $CHCl_3$ and the substrate was added. Mesitylene was used as internal standard. After the experiment temperature was reached *tert*-butylhydroperoxide was added to start the reaction and aliquots for GC–MS measurements were withdrawn at given time intervals. The GC samples were quenched with MnO_2, diluted with ethyl acetate and measured. All yields obtained by GC have an esd of ± 5%.

5.6. DFT modelling details

The reported calculations were performed with the hybrid meta exchange–correlation functional M06 [56], as implemented by the Gaussian 09 program package [57]. The Mo atom was described by Stuttgart-Dresden effective core potentials (ECP) and an SDD basis set [58], while a 6-31G(d') basis set was employed for the remaining atoms [59]. All computations were performed using an ultrafine grid and Grimmes' dispersion correction [60].

The reported geometries for the isomers of complex **1** (species **A** and **B**) represent fully optimized ground states (positive eigenvalues). The computed frequencies were used to make zero-point and thermal corrections to the electronic energies; the reported free energies are quoted in kcal/mol relative to the specified standard. The geometry-optimized structures presented here have been drawn with the *JIMP*2 molecular visualization and manipulation program [61].

5.7. Crystallography

X-ray crystallographic measurements were carried out at 170 K (**2** and **3**) or at 120 K (**5**) according to the ω-scan method on a Nonius KappaCCD diffractometer using Mo-Kα radiation (λ = 0.71073 Å). The Denzo Scalepack program packages were used for cell refinements and data reductions. SADABS absorption correction [62] was applied for the data of all compounds. The structures were solved by direct methods, using SHELXS-97 [63] or SUPERFLIP [64] programs with the WinGX [65] graphical user interface. Structural refinements were carried out using SHELX-97 [66].

CRediT authorship contribution statement

Md Kamal Hossain: Investigation, Writing - original draft, Writing - review & editing. **Jörg A. Schachner:** Investigation, Writing - original draft. **Matti Haukka:** Investigation. **Michael G. Richmond:** Investigation, Writing - original draft. **Nadia C. Mösch-Zanetti:** Supervision, Writing - original draft. **Ari Lehtonen:** Supervision, Writing - original draft. **Ebbe Nordlander:** Conceptualization, Supervision, Writing - review & editing, Project administration, Funding acquisition.

Declaration of Competing Interest

The authors declare that they have no known competing financial interests or personal relationships that could have appeared to influence the work reported in this paper.

Acknowledgements

We gratefully acknowledge financial support from the COST Action CM1003 *Biological oxidation reactions-mechanisms and design of new catalysts*. MGR thanks the Robert A. Welch Foundation (Grant B-1093) for funding. The DFT calculations were performed at UNT through CASCaM, which is an NSF-supported facility (CHE-1531468). M.K.H. thanks the European Commission for an Erasmus Mundus predoctoral scholarship and Dr. Arun Kumar Raha for experimental assistance.

Appendix A. Supplementary data

Supplementary data to this article can be found online at https://doi.org/10.1016/j.poly.2021.115234.

References

[1] A. Thapper, A. Behrens, J. Fryxelius, M.H. Johansson, F. Prestopino, M. Czaun, D. Rehder, E. Nordlander, Dalton Trans. (2005) 3566.
[2] M.J. Romão, Dalton Trans. (2009) 4053.
[3] R. Hille, Chem. Rev. 96 (1996) 2757.
[4] R. Hille, Met. Ions Biol. Syst. 39 (2002) 187.
[5] R. Hille, T. Nishino, F. Bittner, Coord. Chem. Rev. 255 (2011) 1179.
[6] R. Mayilmurugan, B.N. Harum, M. Volpe, A.F. Sax, M. Palaniandavar, N.C. Mösch-Zanetti, Chem. Eur. J. 17 (2011) 704.
[7] B.L. Tran, C.J. Carrano, Inorg. Chem. 46 (2007) 5429.
[8] A.C. Ghosh, P.P. Samuel, C. Schulzke, Dalton Trans. 46 (2017) 7523.
[9] M. Ahmadi, C. Fischer, A.C. Ghosh, C. Schulzke, Front. Chem. 7 (2019) 486.
[10] J. Paudel, A. Pokhrel, M.L. Kirk, F. Li, Inorg. Chem. 58 (2019) 2054.
[11] A.J. Millar, C.J. Doonan, P.D. Smith, V.N. Nemykin, P. Basu, C.G. Young, Chem. Eur. J. 11 (2005) 3255.
[12] M.C. Reis, M. Marín-Luna, C.S. Lopez, O.N. Faza, Inorg. Chem. 56 (2017) 10570.
[13] C.G. Young, Eur. J. Inorg. Chem. (2016) 2357.
[14] P. Basu, B.W. Kail, A.K. Adams, V.N. Nemykin, Dalton Trans. 42 (2013) 3071.
[15] T. Schindler, A. Sauer, T.P. Spaniol, J. Okuda, Organometallics 37 (2018) 4336.
[16] A. Thapper, R.J. Deeth, E. Nordlander, Inorg. Chem. 41 (2002) 6695.
[17] M.C. van Severen, M. Andrejić, J. Li, K. Starke, R.A. Mata, E. Nordlander, U. Ryde, J. Biol. Inorg. Chem. 19 (2014) 1165.
[18] J. Li, U. Ryde, Inorg. Chem. 53 (2014) 11913.
[19] G. Dong, U. Ryde, J. Inorg. Biochem. 171 (2017) 45.
[20] L. Balapoor, R. Bikas, M. Dargahi, Inorg. Chim. Acta 510 (2020) 119734.
[21] M.K. Hossain, J.A. Schachner, M. Haukka, N.C. Mösch-Zanetti, E. Nordlander, A. Lehtonen, Inorg. Chim. Acta 486 (2019) 17.
[22] E. Topić, J. Pisk, D. Agustin, M. Jendrlin, D. Cvijanović, V. Vrdoljak, M. Rubčić, New J. Chem. 44 (2020) 8085.
[23] J. Pisk, M. Rubčić, D. Kuzman, M. Cindrić, D. Agustin, V. Vrdoljak, New J. Chem. 43 (2019) 5531.
[24] N. Zwettler, M.A. Ehweiner, J.A. Schachner, A. Dupé, F. Belaj, N.C. Mösch-Zanetti, Molecules 2019 (1814) 24.
[25] A. de León, J. García-Antón, J. Ros, G. Guirado, I. Gallardo, J. Pons, New J. Chem. 37 (2013) 1889.
[26] V. Bizet, C.M.M. Hendriks, C. Bolm, Chem. Soc. Rev. 44 (2015) 3378.
[27] E. Wojaczyńska, J. Wojaczyński, Chem. Rev. 120 (2020) 4578.
[28] G.D. Faveri, G. Ilyashenko, M. Watkinson, Chem. Soc. Rev. 40 (2011) 1722.
[29] Y. Shen, P. Jiang, P.T. Wai, Q. Gu, W. Zhang, Catalysts 9 (2019) 31.
[30] S.A. Hauser, M. Cokoja, F.E. Kühn, Catal. Sci. Technol. 3 (2013) 552–561.
[31] F. Cavani, J.H. Teles, ChemSusChem 2 (2009) 508.
[32] P. Traar, J.A. Schachner, B. Stanje, F. Belaj, N.C. Mösch-Zanetti, J. Mol. Catal. A Chem 385 (2014) 54.
[33] S. Gago, J.E. Rodríguez-Borges, C. Teixeira, A.M. Santos, J. Zhao, M. Pillinger, C.D. Nunes, Z. Petrovski, T.M. Santos, F.E. Kühn, C.C. Romão, I.S. Gonçalves, J. Mol. Catal. A: Chem. 236 (2005) 1.
[34] N. Baig, V.K. Madduluri, A.K. Sah, RSC Adv. 6 (2016) 28015.
[35] C.J. Carrasco, F. Montilla, E. Álvarez, C. Mealli, G. Mancac, A. Galindo, Dalton Trans. 43 (2014) 13711.
[36] D. Rehder, Future Med. Chem. 4 (2012) 1823.
[37] J. Hakala, R. Sillanpää, A. Lehtonen, Inorg. Chem. Commun. 21 (2012) 21.
[38] F. Romano, A. Linden, M. Mba, C. Zonta, G. Licini, Adv. Synth. Catal. 352 (2010) 2937.
[39] M. Bagherzadeh, L. Tahsini, R. Latifi, A. Ellern, L.K. Woo, Inorg. Chim. Acta 361 (2008) 2019.
[40] A. Thapper, C. Lorber, J. Fryxelius, A. Behrens, E. Nordlander, J. Inorg. Biochem. 79 (2000) 67.
[41] Z. Zheng, G. Zhao, R. Fablet, M. Bouyahyi, C.M. Thomas, T. Roisnel, O. Casagrande Jr, J.-F. Carpentier, New J. Chem. 32 (2008) 2279.
[42] C.L. Hartley, R.J. DiRisio, T.Y. Chang, W. Zhang, W.R. McNamara, Polyhedron 114 (2016) 133.
[43] J.-B. Wang, L.-P. Lu, J.-Y. Liua, Y.-S. Li, Dalton Trans. 43 (2014) 12926.
[44] J. Andrez, G. Bozoklu, G. Nocton, J. Pécaut, R. Scopelliti, L. Dubois, M. Mazzanti, Chem. Eur. J. 21 (2015) 15188.
[45] E.J. O'Neila, H. Jianga, B.D. Smith, Supramol. Chem. 25 (2013) 315.
[46] R. Mayilmurugan, K. Visvaganesan, E. Suresh, M. Palaniandavar, Inorg. Chem. 48 (2009) 8771.
[47] S. Ito, M. Suzuki, T. Kobayashi, H. Itoh, A. Harada, S. Ohba, Y. Nishida, J. Chem. Soc., Dalton Trans. (1996) 2579.
[48] R. Viswanathan, M. Palaniandavar, T. Balasubramanian, T.P. Muthiah, Inorg. Chem. 37 (1998) 2943.
[49] M.E. Judmaier, A. Wallner, G.N. Stipicic, K. Kirchner, J. Baumgartner, F. Belaj, N. C. Mösch-Zanetti, Inorg. Chem. 48 (2009) 10211.
[50] B.E. Schultz, S.F. Gheller, M.C. Muetterties, M.J. Scott, R.H. Holm, J. Am. Chem. Soc. 115 (1993) 2714.
[51] L.M. Thomson, M.B. Hall, J. Am. Chem. Soc. 123 (2001) 3995.
[52] A. Peuronen, R. Sillanpää, A. Lehtonen, ChemistrySelect 3 (2018) 3814.
[53] C.J. Hinshaw, D. Peng, R. Singh, J.T. Spence, J.H. Enemark, M. Bruck, J. Kristofzski, S.L. Merbs, R.B. Ortega, P.A. Wexler, Inorg. Chem. 28 (1989) 4483.
[54] C.J. Whiteoak, G.J.P. Britovsek, V.C. Gibson, A.J.P. White, Dalton Trans. (2009) 2337.
[55] (a) J. Topich, J.O. Bachert III, Inorg. Chem. 31 (1992) 511 (b) J. Topich, J.T. Lyon III, Inorg. Chem., 23 (1984) 3202.
[56] Y. Zhao, D.G. Truhlar, Theor. Chem. Acc. 120 (2008) 215.
[57] M.J. Frisch, G.W. Trucks, H.B. Schlegel, G.E. Scuseria, M.A. Robb, J.R. Cheeseman, G. Scalmani, V. Barone, B. Mennucci, G.A. Petersson, H. Nakatsuji, M. Caricato, X. Li, H. P. Hratchian, A.F. Izmaylov, J. Bloino, G. Zheng, J.L. Sonnenberg, M. Hada, M. Ehara, K. Toyota, R. Fukuda, J. Hasegawa, M. Ishida, T. Nakajima, Y. Honda, O. Kitao, H. Nakai, T. Vreven, J. A. Montgomery, Jr., J.E. Peralta, F. Ogliaro, M. Bearpark, J.J. Heyd, E. Brothers, K.N. Kudin, V.N. Staroverov, R. Kobayashi, J. Normand, K. Raghavachari, A. Rendell, J.C. Burant, S.S. Iyengar, J. Tomasi, M. Cossi, N. Rega, J.M. Millam, M. Klene, J.E. Knox, J.B. Cross, V. Bakken, C. Adamo, J. Jaramillo, R. Gomperts, R.E. Stratmann, O. Yazyev, A.J. Austin, R. Cammi, C. Pomelli, J.W. Ochterski, R.L. Martin, K. Morokuma, V.G. Zakrzewski, G.A. Voth, P. Salvador, J.J. Dannenberg, S. Dapprich, A. D. Daniels, O. Farkas, J.B. Foresman, J.V. Ortiz, J. Cioslowski, D.J. Fox, Gaussian 09, Revision A.02, Gaussian, Inc., Wallingford CT, 2009.
[58] D. Andrae, U. Haeussermann, M. Dolg, H. Stoll, H. Preuss, Theor. Chim. Acta 77 (1990) 123.
[59] (a) G.A. Petersson, A. Bennett, T.G. Tensfeldt, M.A. Al-Laham, W.A. Shirley, J. Mantzaris, J. Chem. Phys. 89 (1988) 2193;
(b) G.A. Petersson, M.A. Al-Laham, J. Chem. Phys. 94 (1991) 6081.
[60] S. Grimme, S. Ehrlich, L. Goerigk, J. Comp. Chem. 32 (2011) 1456.
[61] (a) JIMP2, version 0.091, a free program for the visualization and manipulation of molecules: M.B. Hall, R.F. Fenske, Inorg. Chem. 11 (1972) 768; (b) J. Manson, C.E. Webster, M.B. Hall, Texas A&M University, College Station, TX, 2006: http://www.chem.tamu.edu/jimp2/index.html.
[62] G.M. Sheldrick, SADABS, University of Göttingen, Germany, 2008.
[63] G.M. Sheldrick, SHELXS-97, Program for Crystal Structure Determination, University of Göttingen, Germany, 1997.
[64] L. Palatinus, G. Chapuis, J. Appl. Crystallogr. 40 (2007) 786.
[65] L.J. Farrugia, J. Appl. Crystallogr. 32 (1999) 837.
[66] G.M. Sheldrick, Acta Crystallogr. Sect. A: Found. Crystallogr. 64 (2008) 112.